Random walker's view of networks whose growth it shapes

Robert J. H. Ross,[*] Charlotte Strandkvist,[†] and Walter Fontana[‡]
Department of Systems Biology, Harvard Medical School, 200 Longwood Avenue, Boston, Massachusetts 02115, USA

(Received 7 December 2018; published 14 June 2019)

We study a simple model in which the growth of a network is determined by the location of one or more random walkers. Depending on walker motility rate, the model generates a spectrum of structures situated between well-known limiting cases. We demonstrate that the average degree observed by a walker is a function of its motility rate. Modulating the extent to which the location of node attachment is determined by the walker as opposed to random selection is akin to scaling the speed of the walker and generates new limiting behavior. The model raises questions about energetic and computational resource requirements in a physical instantiation.

DOI: 10.1103/PhysRevE.99.062306

I. INTRODUCTION

A large body of literature is devoted to analyzing systems that can be modeled as growing networks [1–4]. In many cases network growth is coupled to a process situated on the network. Systems of this kind include the developing brain whose action potentials help shape neuronal architecture [5], social networks whose evolution is driven by interactions between the very individuals that constitute these networks, technological innovation which depends on current technologies within reach, and the internet whose structure is, among other things, determined by its usage [6]. Inspired by these real-world systems, we present a network growth model in which a local process situated on a network coordinates the network's growth. We also examine how coupling a local process situated on the network and the growth of this network can constrain the behavior of this local process. Indeed, it has been recently demonstrated that coupling a local process to network growth can bound the entropy associated with processes such as diffusion [7].

We study a simple network growth mechanism that is driven by a local process situated on the network. Our focus is to compare and relate the global view of the network with the local view of the network as accessible to a process situated on it. Many of the most influential network growth algorithms operate from a global perspective; that is, the entire network, or a statistic associated with it, is utilized in determining a growth event. For instance, the Barabási-Albert growth algorithm requires knowledge of the global network structure. Similarly, exponential networks, and other more realistic models of network growth, sample the location of a growth event from the entire network [8]. These issues have been previously noted [9–12], but it remains unclear when global growth strategies can be implemented by local processes subject to realistic constraints. Comparing local and global views will sharpen this question. To this end, we extend previous studies by using an exceedingly simplified local growth model based on a random walker. We focus on the expected degree of the node at which the walker is situated when a growth event occurs and demonstrate that for our local growth model it is a function of the walker motility rate. This is in contrast to nongrowing networks, whereby the expected degree observed by a walker does not depend on the walker motility rate in the long-time limit. This simple approach allows us to obtain conclusions regarding the degree distributions that can be generated by this model and characterize canonical differences between global growth algorithms and algorithms enacted by local processes situated on the network.

II. MODEL AND RESULTS

We denote the number of nodes in the network at time t with $V(t) \in \mathbb{N}$ and the number of edges with $E(t) \in \mathbb{N}$. $V(t) = N(t) + N_0$, where $N(t)$ is the number of growth events that occurred up to time t and N_0 is the number of nodes in the seed network. Each node i is uniquely and permanently labeled at its creation by the count of growth events that have occurred up to and including its creation. Thus, $i \in \{1, 2, \ldots, V(t)\}$, with the last node labeled $V(t)$. The degree of node i is denoted by k_i.

In "walker-induced network growth" (WING) a random walker situated on the network moves with a rate per time unit, r_W. In WING time is evolved continuously, in accordance with the Gillespie algorithm [13], such that random walker movement and network growth events are modeled as exponentially distributed "reaction events" in a Markov chain. We employ a stochastic network growth mechanism in which the addition of a new (nonoccupied) node occurs with rate r_N per unit time. Network growth is therefore linear. At each growth event, a single node forms an edge with the node upon which the random walker is located. This means that just after addition to the network, new nodes are of degree $k = 1$. There is no limit to the number of nodes from which the network can be composed. We typically start the process with a fully connected network of N_0 nodes and a randomly chosen

[*]robert_ross@hms.harvard.edu
[†]charlotte_strandkvist@hms.harvard.edu
[‡]walter_fontana@hms.harvard.edu

position of the walker (although our results do not hinge on this choice).

The model can be extended in any number of ways, and we shall consider two in particular. In one extension, the network hosts $m \leqslant N_0$ walkers. When $m > 1$, the walkers exclude each other in the sense that if a walker attempts to move to an already occupied node, the movement is aborted. The new node is connected to all m distinct locations of the walkers and has therefore degree m. Networks generated with a single walker are asymptotically trees, whereas networks shaped by multiple walkers contain cycles. The other extension introduces a parameter α, which modulates the coupling between walker and growth. With probability α, growth occurs at the location of the walker as just described, and with probability $1-\alpha$ the new node is linked to a random location in the network.

Given an arbitrary initial network and in the absence of network growth ($r_N = 0$), it is well known that, in the long-time limit, the probability p_i of finding a random walker at node i is proportional to its degree k_i, $p_i = k_i/\sum_j k_j = k_i/(2E)$, with E the number of edges in the network. This result is independent of the walker motility rate in the long-time limit, so long as the motility rate is greater than zero. Barabási and Albert (BA) considered a growing network [14], where growth occurs by repeatedly attaching a new node of degree 1 to a node i chosen according to $p_i(g) = k_i/[2E(g)]$ with g indicating the growth step. This process, known as preferential attachment, was proposed as a mechanism for generating scale-free networks characterized by a power-law degree distribution $p(k) \sim k^{-\gamma}$. It was shown in Refs. [8,15] that the BA procedure results in $p_{BA}(k) = 4/[k(k+1)(k+2)]$. Preferential attachment hinges on a global view of the network, because it utilizes knowledge of the entire network at every step g. This prompted Saramäki and others [9,10] to propose a model in which random walkers sample the local connectivity of the growing network and serve as attachment points for the addition of a new node. The WING model shares the spirit of this approach but is simpler and designed to study (1) how coupling an autonomous network growth to one or more random walkers on the network can yield networks of different kinds and (2) how a network so constructed might be described from the walker's point of view.

A. Single walker, $m = 1$

As expected, the network structures formed by the WING model depend on the ratio $r = r_W/r_N$ (Fig. 1). When $r_W = 0$, the walker does not move from its initial position on the network, and each new node therefore links to the same node, generating a "star" structure [Fig. 1(a)]. In the limit $r = r_W/r_N \to \infty$ the probability of finding the random walker at node i becomes $p_i(t) = k_i/[2E(t)]$, that is, determined solely by the degree of node i, and so results in the BA case [Fig. 1(d)]. This behavior is reflected in the degree distributions generated as r sweeps across its range, as shown in Fig. 2. It can be seen, perhaps surprisingly, that even at $r = 100$ the BA degree distribution is already well approximated by WING. In the Supplemental Material [16] we further examine the discrepancy between these two degree distributions. The main observations are the following: (1) At small r, the degree distribution is closer to an exponential, $p(k) \sim \exp(\beta k)$—we expand on this point in the Supplemental Material [16]—and approaches the power law of the BA case, $p_{BA}(k)$, as r grows large. (2) Stationarity, i.e., a degree distribution independent of network size, is attained relatively quickly. (3) Figure 3 points to an interesting property of WING: a linear dependence between the average graph distance between two nodes i and j and their age difference, independent of network size. Distance is defined as usual in terms of the number of edges separating two nodes, while the age of a node i is its label $N(i)$, a linear function of continuous time, and the age difference between two nodes i and j is $|N(j) - N(i)|$. The distance between nodes is maximized between $r_W = 0.5$ and $r_W = 1$. This "big-world" property of the network is not observed for either the BA model or growing exponential models [8] and is due to the local implementation of the WING algorithm. In the Supplemental Material [16] we present degree distributions generated by WING when the network is grown by two walkers, $m = 2$.

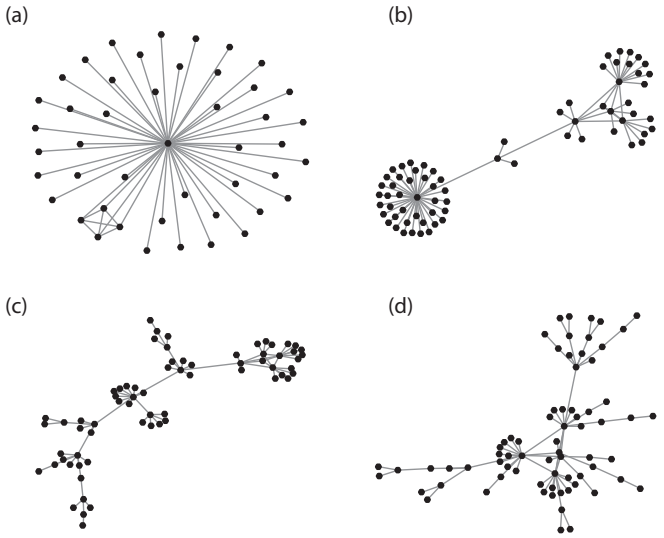

FIG. 1. Networks created by WING. The motility rate, r_W, of the only walker differs across panels, while the network growth rate is constant $r_N = 1$. For the sake of less congestion, simulations are stopped after $t = 50$ time units. The seed network is a fully connected set of $N_0 = 5$ nodes, still recognizable as the only clique. (a) $r_W = 0$; (b) $r_W = 0.1$; (c) $r_W = 1$; (d) $r_W = 100$.

Because the walker shapes the growth of the network on which it moves, it is of interest to describe the network from the viewpoint of the walker. One way of doing so is to compute the average degree of the node the walker is situated at when a growth event occurs, as distinct from the average degree of a node given the network as a whole. We denote the walker's point of view with $\langle k_W \rangle$ and the global point of view with $\langle k \rangle$, where $\langle k \rangle$ is asymptotically a constant that is independent of the motility rate of the random walker. We assume that WING attains a stationary degree distribution in the $N(t) \to \infty$ limit. This assumption is justified in the Supplemental Material [16].

Let $p_W(k)$ be the probability that the walker is situated at a node of degree k when a growth event occurs. To obtain $p_W(k)$ numerically we record the trace (sequence) τ_r of degrees seen

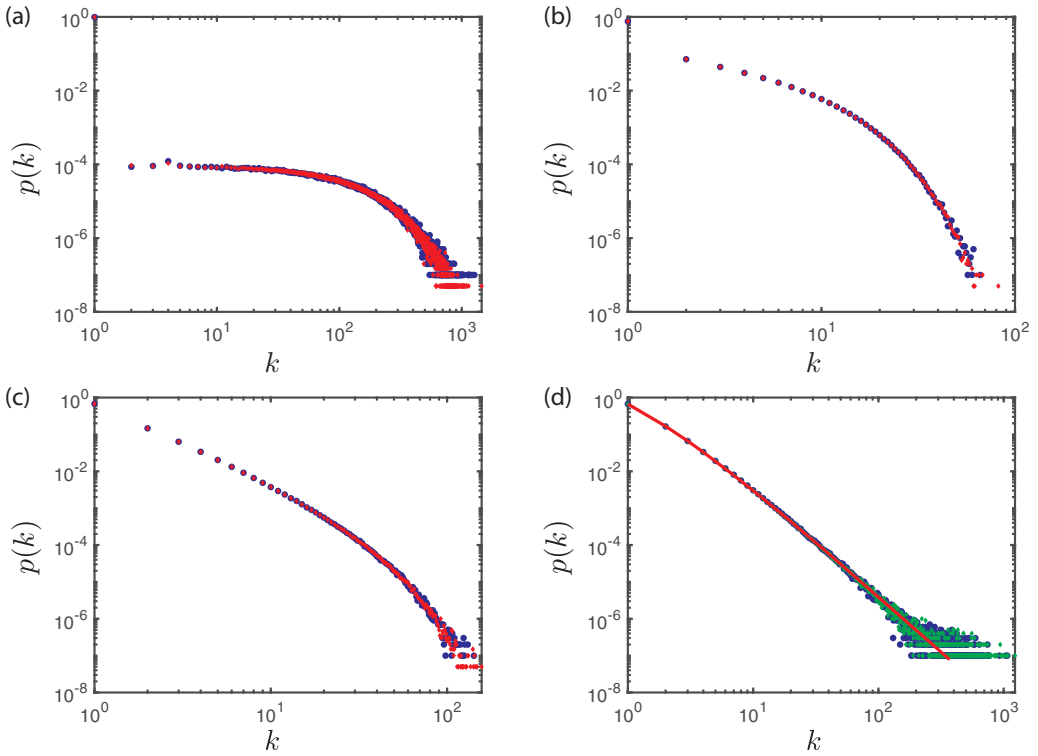

FIG. 2. Degree distributions generated by WING. The panels are for different r_W values. For all panels $r_N = 1$, $m = 1$, and averages are taken over 1000 replicates. (a) $r_W = 0.01$; (b) $r_W = 1$; (c) $r_W = 10$; (d) $r_W = 100$. In panels (a)–(c), simulations were run to $t_1 = 100\,000$ (blue circles) and to $t_2 = 200\,000$ (red diamonds), indicating stationarity. In panel (d), representing the large-r case, we compare the WING model (blue circles) with the BA procedure ($r_W \sim \infty$, green diamonds) at $t = 100\,000$. The red line is $p_{BA}(k) = 4/[k(k+1)(k+2)]$ as per Refs. [8,15].

by the walker in a simulation r, collect the frequency with which the degree is k at event g across replicate traces τ_r (r indexing the replicate) each comprising N growth events, and average over g. Specifically, denoting the degree the walker observes at event g of trace τ_r by $\tau_{r,g}$, we have

$$p_W(k,g) = \frac{1}{R}\sum_{r=1}^{R}\delta(k-\tau_{r,g}),$$
$$p_W(k) = \frac{1}{V}\sum_{g=1}^{V} p_W(k,g), \tag{1}$$

where $\delta(x) = 1$ if $x = 0$ and $\delta(x) = 0$ otherwise. The global degree distribution $p(k)$ is computed likewise, but instead of observing a single node at growth event g, we observe all nodes in the network; thus, $p(k, g)$ is the probability of degree k in a network at growth step g. Figure 4 depicts $p_W(k)$ and $p(k)$ for $r = 1$. Other values of r generate similar plots (not shown).

We can express $\langle k_W \rangle$ as a function of global moments. Let $n(k, g)$ denote the average number of nodes of degree k in a network when the gth growth event occurs. If $p(k)$ is stationary, $n(k, g) = g\,p(k)$. The change in $n(1, g)$ across a growth event is given by

$$n(1,g+1) - n(1,g) = (g+1)p(1) - gp(1)$$
$$= p(1) = 1 - p_W(1), \tag{2}$$

where the last equation follows because a growth event always adds one new node of degree 1 and one node of degree 1 is lost only if the walker is located at a degree-1 node, which

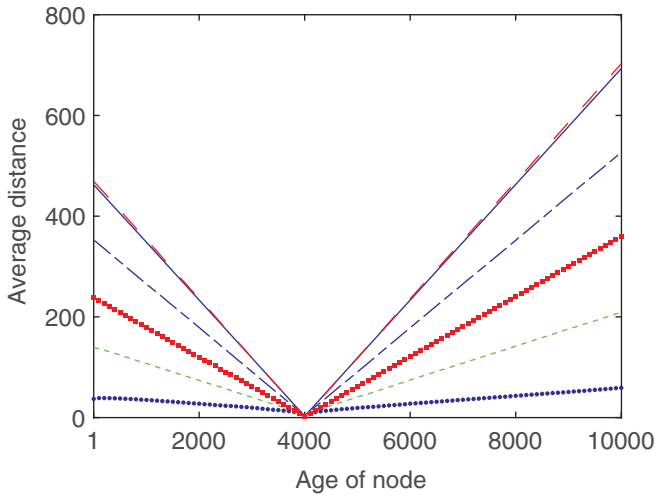

FIG. 3. Distance between nodes as a function of age. The average distance between a node of age 4000 and all other nodes in a network generated with WING is shown as a function of their age difference for different values of walker motility. $r_W = 10$ (blue disks), $r_W = 5$ (green dashed), $r_W = 2$ (blue dot-dashed), $r_W = 1$ (blue solid), $r_W = 0.5$ (red dashed), and $r_W = 0.1$ (red squares). $N = 10\,000$.

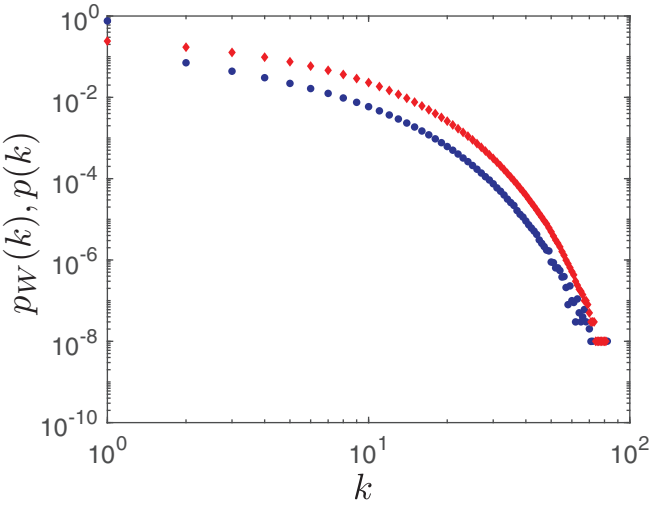

FIG. 4. The local degree distribution. $p(k)$ (blue disks) is compared with $p_W(k)$ (red diamonds) after $N = 10\,000$ growth events. Convergence of $p_W(k)$ to a stationary distribution is fast. $r_W = 1$, $r_N = 1$.

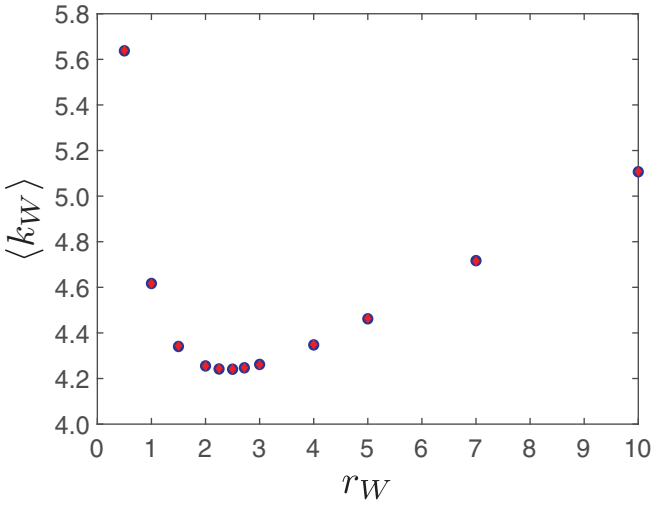

FIG. 5. The view from the walker. The red diamonds show $\langle k_W \rangle$ obtained directly by simulation, and the blue disks show $\langle k_W \rangle$ obtained from (4) with $\langle k^2 \rangle$ obtained from simulation. The second moment, $\langle k_W^2 \rangle$, is shown in the Supplemental Material [16]. $r_N = 1$, $N = 10\,000$, and $R = 100\,000$ replicates.

happens with probability $p_W(1)$. Likewise, one node of degree 2 is gained only if the walker is located at a degree-1 node and lost only if the walker is located at degree-2 node, yielding a net average change of $p(2) = p_W(1) - p_W(2)$. In general, we have the balance equations:

$$p(k) = p_W(k-1) - p_W(k), \quad k > 1. \tag{3}$$

From (2) and (3) we calculate the expected global degree, $\langle k \rangle = 2$. In a similar fashion we obtain $\langle k^2 \rangle = 2\langle k_W \rangle + 2$ and, thus,

$$\langle k_W \rangle = \tfrac{1}{2}(\langle k^2 \rangle - 2). \tag{4}$$

Equation (4) is similar to a well-known result for nongrowing networks in which the probability of a walker being at a node depends only on the node's degree [17,18]. In contrast, in WING the probability of a walker being at a node does not depend solely on its degree, and so $\langle k_W \rangle$ becomes a function of the motility rate of the walker (Fig. 5). For the second moment from the walker's perspective we obtain in a similar fashion

$$\langle k_W^2 \rangle = \tfrac{1}{6}\big(2\langle k^3 \rangle - 3\langle k^2 \rangle + 2\big). \tag{5}$$

In the Supplemental Material [16] we provide the balance equations for generalizing these results to m self-excluding walkers:

$$\begin{aligned} \langle k \rangle &= 2m, \\ \langle k_W \rangle &= \frac{1}{2}\frac{\langle k^2 \rangle - m(m+1) + 2}{m}, \\ \langle k_W^2 \rangle &= \frac{1}{3}\frac{\langle k^3 \rangle - m^3 - m - 3m\langle k_W \rangle}{m}, \end{aligned} \tag{6}$$

where we used $\langle k_W \rangle$ to describe $\langle k_W^2 \rangle$ for brevity. We will address multiple walkers later in the paper.

Together with Fig. 5, Eqs. (4) and (5) permit a few observations: (1) $\langle k_W \rangle$ is finite for $0 < r_W < \infty$. (2) $\langle k_W \rangle$ diverges in both limits $r_W \to \infty$ and $r_W \to 0$. As $r_W \to \infty$ in the limit the probability of the walker being at a node depends solely on its degree, and so WING approaches the BA procedure, which yields power law $p_{BA}(k)$ with divergent $\langle k^2 \rangle$. In the limit $r_W \to 0$, the walker is pinned and generates a star network with a single node of divergent degree. (3) Since $\langle k_W \rangle$ is a convex function of r_W, oscillations could be generated by a mechanism in which the walker's motility is a function of the observed mean degree. Moreover, $\langle k_W \rangle$ is minimized when $\langle k^2 \rangle$ is minimized. A more sophisticated walker could achieve this minimization by employing a gradient descent with respect to its own motility. (4) A given $\langle k_W \rangle$ can be attained with a pair of distinct r_W values, which, by (4), yield global $p(k)$ distributions with the same $\langle k^2 \rangle$ (and variance, since $\langle k \rangle = 2$ always). Yet these r_W values do not yield the same $\langle k_W^2 \rangle$, as seen in Fig. S1 in the Supplemental Material [16], and hence the $p(k)$ distributions must differ in the third moment $\langle k^3 \rangle$ by virtue of (5). We finally demonstrate that for $0 \leqslant r_W < \infty$ the WING model cannot generate a Barabási-Albert network with stationary degree distribution $p_{BA}(k)$, as already suggested by Fig. 2. Let $w = r_W/(r_W + r_N)$ and $g = r_N/(r_W + r_N)$ denote the probabilities that the next event is either a step by the walker or the growth of the network, respectively. Furthermore, let $p_{N(t)}$ denote the probability that, when a growth event occurs, the random walker is located at the last node added to the network. If the stationary distribution were $p_{BA}(k)$, $p_{N(t)}$ would tend to zero in the limit $t \to \infty$ [i.e., $N(t) \to \infty$], because all nodes in the network must be visited proportional to their degree. Hence, $p_{N(t)}$ must vanish. Yet, for $r_W < \infty$, $p_{N(t)}$ is bounded below:

$$p_{N(t)} > \sum_{k=1}^{\infty} p_W(k)\, g\, \frac{w}{k+1}. \tag{7}$$

The right-hand side represents the network-size independent probability of just one scenario for the walker to be positioned on the last node added: the walker is at a node of degree k,

a growth event occurs, and the walker moves to the added node. Clearly there are many more ways for the walker to reach that node before the next growth event occurs. However, a lower bound for $p_{N(t)}$ contradicts its vanishing implied by the assumption that $p_{BA}(k)$ is the global stationary degree distribution. Hence, $p_{BA}(k)$ cannot be the stationary degree distribution for WING for any $r_W < \infty$.

B. Variable coupling α

We next refine the WING model by adding a parameter $0 \leqslant \alpha \leqslant 1$ that tunes the influence of the walker on network growth: A growth event links the new node with probability α to the location of the walker and with probability $1-\alpha$ to a node chosen uniformly at random from the network, which includes the location of the walker. The case described so far corresponds to $\alpha = 1$. Modulating α in this manner allows us to explore network growth algorithms that contain both global and local aspects in their computation. It is important to emphasize here that the manner in which we a select a node with probability $1-\alpha$ is irrelevant, as long as we sample over all nodes in the network, that is, globally. For instance, implementing a preferential attachment model instead of this random attachment model would not qualitatively change the results we present.

Following the same reasoning of the last section, we compute the first and second moments of the distribution $p_W(k,\alpha)$ observed by the walker as a function of α:

$$\langle k_W(\alpha)\rangle = \frac{1}{2\alpha}(\langle k^2(\alpha)\rangle + 4\alpha - 6), \tag{8}$$

$$\langle k_W^2(\alpha)\rangle = \frac{1}{3\alpha}\left[\langle k^3(\alpha)\rangle + 3\langle k^2(\alpha)\rangle\left(\alpha - \frac{3}{2}\right) + 1\right]. \tag{9}$$

In Fig. 6 we compare (8) for different network sizes V. The following observations stand out for the modified WING model: (1) Fig. 6 indicates that convergence for $\alpha < 1$ at high walker motility is slow compared to $\alpha = 1$ or low walker motility. (2) The dotted line in Fig. 6 is Fig. 5 with the abscissa scaled by a factor of 2: the average degree seen by the walker at speed r_W when growth always occurs at the location of the walker is the same as that seen by a walker with half that speed when growth occurs half the time at the location of the walker and half the time at a random location. This suggests that

$$\langle k_W(\alpha_1 = 1, r_W)\rangle = \langle k_W(\alpha_2, r_W\alpha_2)\rangle, \tag{10}$$

where the dependency on r_W is made explicit and $r_N = 1$. As network size $V(t) \to \infty$ in the limit, the probability that a growth event occurs at the location of the walker tends to α, since it becomes increasingly unlikely that any random growth events, occurring with probability $1-\alpha$, hit the walker's location by chance. The walker can therefore be viewed as having an effective motility or α horizon $\hat{r}_W = r_W/\alpha$. We can rephrase (10) as asserting that the fraction $1-\alpha$ of growth events do not affect, in the large $V(t)$ limit, the world that the walker sees within its "α horizon." (3) It follows that

$$\lim_{\alpha\to 0}\langle k_W(\alpha)\rangle \to \infty, \tag{11}$$

which means the effective motility of the walker diverges in the limit $\alpha \to 0$, yielding the BA procedure with a divergent second global moment and therefore a divergent $\langle k_W(\alpha)\rangle$ as in the case of $\alpha = 1$ and $r_W \to \infty$. (iv) The behavior as $r_W \to \infty$ and the behavior at $r_W = \infty$ differ when $\alpha < 1$ compared with $\alpha = 1$. From our treatment of the $\alpha = 1$ case and observation (3) above, $\langle k_W\rangle$ diverges for any α as $r_W \to \infty$. However, if we set $r_W = \infty$, the random walk is theoretically treated as always in equilibrium on the network; i.e., there is no concept of an α horizon for the walker at any $\alpha < 1$, and $\langle k_W\rangle$ remains finite due to the fraction $1-\alpha$ of random growth events. For $\alpha = 1$, $\langle k_W\rangle$ diverges.

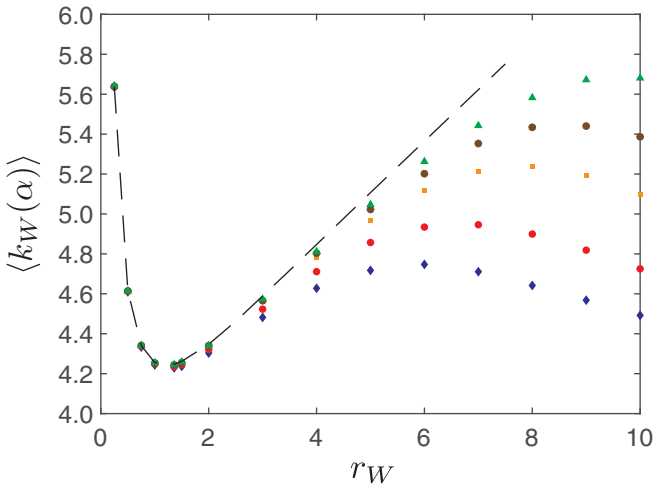

FIG. 6. Tunable walker influence. The graph depicts $\langle k_W(\alpha)\rangle$ as a function of walker motility r_W for different time points (numbers of growth events or, equivalently, network sizes) N, with $r_N = 1$ and $\alpha = 0.5$. Data points are averaged over 10 000 replicates. We obtain the same graphs using both simulation data and (8) (not shown). Blue diamonds: $N = 10\,000$, red disks: $N = 20\,000$, orange squares: $N = 50\,000$, brown asterisks: $N = 100\,000$, green triangles: $N = 200\,000$. The coupling parameter $\alpha = 0.5$ has here half the value it has in Fig. 5. The dashed line is the graph shown in Fig. 5 but plotted against an abscissa scaled by a factor of $1/\alpha = 2$.

C. Two walkers, $m = 2$

We finally examine $\langle k_W\rangle$ when there are two walkers on the network. The behavior in this instance follows naturally from the $m = 1$ case; however, we pay special attention to the way in which the walkers "interfere" with each others perspective, that is $\langle k_W\rangle$, of the network. Figure 7 shows that Eqs. (6) agree extremely well with simulations, which is to be expected given they are exact. Figure 7 and Eqs. (6) permit the following observations: (1) The expected degrees of the nodes at which walker 1 and 2 are located when a growth event occurs, $\langle k_W^{(1)}\rangle$ and $\langle k_W^{(2)}\rangle$, respectively, are not the same as if each walker was on the network alone, or if two nodes of degree $k = 1$ were added to the network for each growth event. It is also apparent from Fig. 7 that $\langle k_W^{(1)}\rangle$ and $\langle k_W^{(2)}\rangle$ have both the same value twice. (2) When $r_W^{(1)} = c$, where c is a constant, and $r_W^{(2)} \to 0$, both $\langle k_W^{(1)}\rangle$ and $\langle k_W^{(2)}\rangle$ diverge in the limit. However, if $r_W^{(1)} = c$ and $r_W^{(2)} = 0$, then only $\langle k_W^{(2)}\rangle$ will diverge and $\langle k_W^{(1)}\rangle$ remains finite. (3) When $r_W^{(1)} = c$ and $r_W^{(2)} = \infty$ (theoretically), both $\langle k_W^{(1)}\rangle$ and $\langle k_W^{(2)}\rangle$ remain finite.

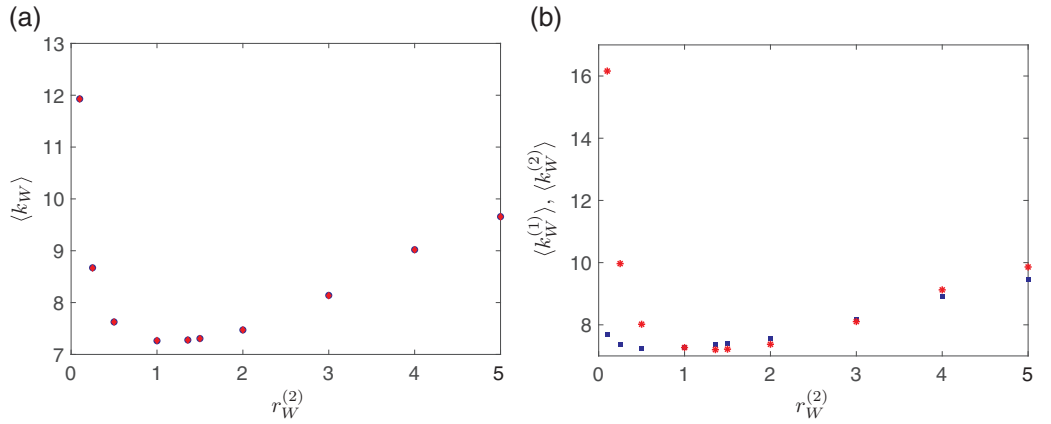

FIG. 7. Multiple walkers. The figure depicts the first moment of the degree distribution observed by two random walkers, 1 and 2, as a function of the movement rate of walker 2. (a) The red diamonds show $\langle k_W \rangle$ averaged over both walkers obtained directly by simulation, and the blue disks show $\langle k_W \rangle$ according to (6) with $m = 2$ and $\alpha = 1$, where $\langle k^2 \rangle$ is obtained from simulation. (b) The mean degree seen by each walker as obtained from simulation directly. In both panels, $r_N = 1$, $N = 2\,000\,000$, and $R = 100$ replicates.

This is also true in the limit when $r_W^{(1)} = c$ and $r_W^{(2)} \to \infty$. (4) Following a growth event the random walkers will "meet" at a constant rate in the limit $N \to \infty$. A lower bound for the probability of this occurring following a growth event can be written as

$$g w^{(1)} \left[\sum_{k=1}^{\infty} \frac{p_W^1(k)}{k+1} \right] w^{(2)} \left[\sum_{k=1}^{\infty} \frac{p_W^2(k)}{k+1} \right], \tag{12}$$

which is independent of N. These observations have obvious analogues when there are more than two walkers on the network.

III. DISCUSSION AND CONCLUSION

We have presented a simple network growth mechanism in which random walkers on a network control where the network grows and thus determine its structure. Many real-world networks exhibit structures that are determined, at least in part, by processes situated on them [6]. Branching processes such as tree growth, blood vessels, the developing nervous system, branching polymers, social networks, and technological structures are all systems that are influenced by intrinsic processes in their growth. Importantly, they are also systems that must be flexible in their structure depending on their particular environment. In the WING model this sensitivity is captured in the "tuning parameter" r, which determines the network structure.

We provided a description of WING by taking the perspective of the walker, expressing the expected degree of the node the walker is situated at when a growth event occurs, $\langle k_W \rangle$, and demonstrating that when $0 < r_W < \infty$, $\langle k_W \rangle$ remains finite. We then extended the model by adding a parameter α controlling the coupling between network growth and walker location, and showed that this gives rise to an effective motility that causes new behavior as $\alpha \to 0$ and $r_W \to \infty$. We finished by addressing the scenario in which there are two walkers present on the network, paying particular attention to how one walker could influence the perspective of the other.

It is important to address whether WING could effectively generate the network constructed by the BA model. That is, given the requirement for the position of the random walker to equilibrate over an increasingly large network, is this energetically feasible? Even though at finite values of r_W the degree distribution associated with the BA model is approximately achieved, as demonstrated by Fig. 2, it seems network growth algorithms that are formulated from a global perspective of the network may require unrealistic behaviors if they are to be enacted by local processes situated on the network. The transition between an algorithm based on global criteria being efficiently implementable by local processes at small but not at large network sizes might also be of interest for identifying whether real-world networks are being built using global knowledge or local processes, or why a network may appear to grow differently once it has exceeded a certain size. The modulation of α allowed us to examine network growth algorithms that utilize both local processes and global knowledge of the network. In this scenario it is apparent that both the degree distribution and the observations of the random walker exhibit prolonged nonequilibrium behavior related to network size (Fig. 6). This is captured, however, only when the finite motility of the random walker is taken into account. A different interpretation would be arrived at if the walker's position was treated at equilibrium on the network, which could be seen to correspond to a global perspective such as that found in the BA model. This observation serves to demonstrate that equilibrium assumptions must be made with caution when applied to local processes known to guide a network's growth.

In view of Fig. 5, it would be interesting to determine the value of r_W at which $\mathrm{d}\langle k_W \rangle / \mathrm{d}r_W = 0$. This the point at which the difference between $\langle k_W \rangle$ and $\langle k \rangle$ is minimized and appears numerically close to Euler's number. More generally, since r_W determines the structure of the network the walker observes, there may be interesting further work into simple mechanisms by which the walker can control what it observes, without resorting to global knowledge. Alternatively, we may ask in what ways an external force can control the observations of a random walker situated on a growing network. For instance, if

α were to be made a function of network size, would a naive random walker be able to discriminate between a change in α and a change in its own motility without recourse to an intrinsic notion of time? Finally, we have studied only how the position of an unbiased random walker evolves, which we did for mathematical ease. However, many other processes could be studied, such as proliferating random walkers of different types interacting on the same growing network [19–21].

ACKNOWLEDGMENT

R.J.H.R. would like to thank Pavel Krapivsky for helpful discussions.

[1] M. A. Porter and J. P. Gleeson, *Dynamical Systems on Networks: A Tutorial*, Frontiers in Applied Dynamical Systems: Reviews and Tutorials, Vol. 4 (Springer, Cham, 2016).

[2] T. Hoffmann, M. A. Porter, and R. Lambiotte, *Temporal Networks* (Springer, Berlin, 2013), pp. 295–313.

[3] P. Holme and J. Saramäki, Phys. Rep. J. **519**, 97 (2012).

[4] N. Perra, A. Baronchelli, D. Mocanu, B. Gonçalves, R. Pastor-Satorras, and A. Vespignani, Phys. Rev. Lett. **109**, 238701 (2012).

[5] M. F. Bear, B. W. Connors, and M. A. Paradiso, *Neuroscience: Exploring the Brain*, 3rd ed. (Lippincott Williams and Wilkins, Philadelphia, 2007).

[6] M. Newman, *Networks: An Introduction* (Oxford University Press, Oxford, 2010).

[7] R. J. H. Ross, C. Strandkvist, and W. Fontana, Phys. Lett. A **383**, 2028 (2019).

[8] S. N. Dorogovtsev, J. F. F. Mendes, and A. N. Samukhin, Phys. Rev. Lett. **85**, 4633 (2000).

[9] J. Saramäki and K. Kaski, Physica A **341**, 80 (2004).

[10] T. S. Evans and J. P. Saramäki, Phys. Rev. E **72**, 026138 (2005).

[11] C. Cannings and J. Jordan, Electron. Commun. Probab. **18**, 77 (2013).

[12] B. Bloem-Reddy and P. Orbanz, J. R. Stat. Soc. B **80**, 871 (2018).

[13] D. T. Gillespie, J. Phys. Chem. **81**, 2340 (1977).

[14] A. L. Barabási and R. Albert, Science **286**, 509 (1999).

[15] P. L. Krapivsky, S. Redner, and F. Leyvraz, Phys. Rev. Lett. **85**, 4629 (2000).

[16] See Supplemental Material at http://link.aps.org/supplemental/10.1103/PhysRevE.99.062306 for details of analytical calculations and further simulation results.

[17] E. van Nimwegen, J. Crutchfield, and M. Huynen, Proc. Natl. Acad. Sci. U. S. A. **96**, 9716 (1999).

[18] B. D. Hughes, *Random Walks and Random Environments* (Oxford: Clarendon Press, Oxford, 1995), Vol. 1.

[19] E. Khain, L. M. Sander, and C. M. Schneider-Mizell, J. Stat. Phys. **128**, 209 (2007).

[20] R. J. H. Ross, R. E. Baker, and C. A. Yates, Phys. Rev. E **94**, 012408 (2016).

[21] R. J. H. Ross, C. A. Yates, and R. E. Baker, Phys. Rev. E **95**, 032416 (2017).

Supplemental Material

A. SECOND MOMENT OF THE LOCAL DEGREE DISTRIBUTION

This Figure accompanies Figure 5 in the main text.

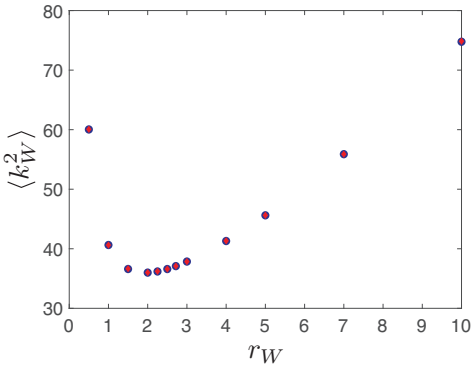

FIG. S1. Second walker moment. The figure depicts the second moment of the degree distribution observed by the random walker as a function of its movement rate. The red diamonds show $\langle k_W^2 \rangle$ obtained directly by simulation and the blue disks show $\langle k_W^2 \rangle$ obtained from equation (5) in the main text with $\langle k^2 \rangle$ and $\langle k^3 \rangle$ obtained from simulation. $r_N = 1$, $N = 10,000$, and $R = 100,000$ replicates.

B. STATIONARITY OF WING

By a stationary degree distribution $p(k)$ we mean that

$$\lim_{N(t)\to\infty} \frac{n(k,t)}{N(t)} \to p(k,t) = p(k) \text{ constant in } t, \tag{S1}$$

where $n(k,t)$ is the number of nodes of degree k in a network of $N(t)$ nodes. We have $n(k,t) = N(t)\,p(k,t)$ and $d\,n(k,t)/dN(t) = p(k,t) + dp(k,t)/dN(t) = p(k,t)$ in the large-$N(t)$ limit. The same reasoning that led to equations (2) and (3) in the main text yields without stationarity assumption

$$\frac{dn(1,t)}{dN(t)} = p(1,t) = 1 - p_W(1,t) \tag{S2}$$

$$\frac{dn(k,t)}{dN(t)} = p(k,t) = p_W(k-1,t) - p_W(k,t),\ k > 1. \tag{S3}$$

As in the main text, these balance equations express that nodes of degree k are lost by linking to the new node at a rate $p_W(k,t)$, the probability that the walker is at a node of degree k just prior to a growth event. For $r_W > 0$, $p_W(1,t)$ cannot go to zero or no nodes of degree 1 would ever be lost, yielding the star network for which $p(1,t) = 1$ for all t, which is attained only when $r_W = 0$. Hence $p_W(1,t)$ is bounded below by some $c_1 wg$. This entails $p_W(k,t) > c_k wg^k$, and by conservation $p_W(k,t) \geq p_W(k+1,t)$. Since by virtue of the lower bounds $p_W(k,t) \to \alpha_k$ as $N(t) \to \infty$, we have that $p(1,t) \to 1 - \alpha_1$, $p(2,t) \to \alpha_1 - \alpha_2$, and so on.

C. MULTIPLE WALKERS

Figure S4 indicates that multiple walkers, $m > 1$, generate stationary degree distributions as in the case of $m = 1$. For multiple walkers with variable α the balance equations read:

$$p(1) = \delta(1-m) - m(1-\alpha)p(1) - m\alpha p_W(1) \tag{S4}$$

$$p(k) = \delta(k-m) + m(1-\alpha)[p(k-1) - p(k)] + m\alpha[p_W(k-1) - p_W(k)], \quad k > 1. \tag{S5}$$

The $\delta(k-m)$ term accounts for the fact that a node of degree m is always added to the network since the incoming node connects to all m walkers.

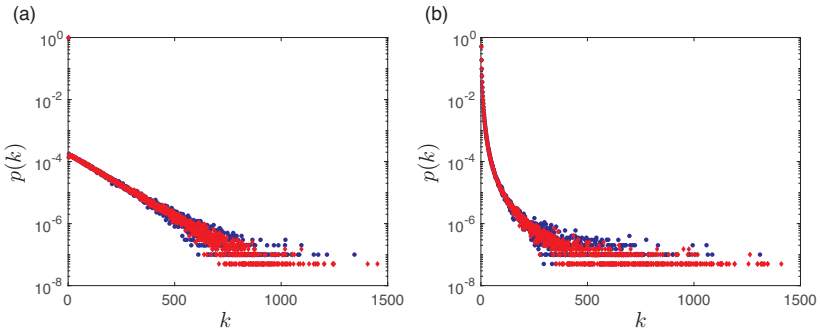

FIG. S2. Degree distribution from multiple walkers. Examples of degree distributions generated by WING dynamics with $m = 2$. Panel (a): $r_W = 0.01$. Panel (b): $r_W = 10$. In all panels $r_N = 1$, $N = 100,000$ (blue disks), $N = 200,000$ (red diamonds); averages from $1,000$ replicates.

D. DEGREE DISTRIBUTION AT LOW r IS CLOSE TO EXPONENTIAL

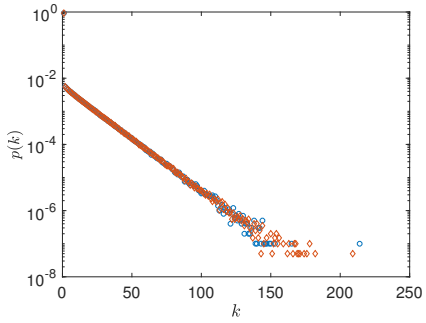

FIG. S3. Degree distributions generated by WING for $r_N = 1$, $m = 1$, and $r_W = 0.1$. Simulations were run to $t_1 = 100,000$ (blue circles) and to $t_2 = 200,000$ (red diamonds). In this instance $\beta \approx -0.0315$ for this value of r.

E. THE DISCREPANCY BETWEEN THE BA AND WING DEGREE DISTRIBUTIONS FOR $r = 100$

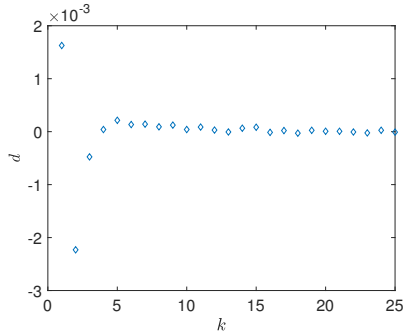

FIG. S4. The discrepancy, $d = p - p_{BA}$, between the BA degree distribution and WING degree distribution for $r = 100$ and $t = 100,000$. It can be seen that the largest discrepancies exist in nodes of degree 1 and degree 2. Nodes of degree 1 occur at a slightly highly probability in the WING model with $r = 100$ ($p(1) \approx 0.668$), as compared to the BA model ($p(1) = 0.\dot{6}$). Nodes of degree 2 occur at a slightly lower probability in the WING model with $r = 100$ ($p(2) \approx 0.164$), as compared to the BA model ($p(1) = 0.1\dot{6}$).